

Characterization of Collagen Abnormalities in Abdominal Aortic Aneurysms

THESIS

Presented in Partial Fulfillment of the Requirements for Honors Research Distinction in
Biomedical Engineering at The Ohio State University

By

Anna Debski

Undergraduate Program in Materials Science and Engineering

The Ohio State University

2020

Thesis Defense Committee:

Professor Gunjan Agarwal, Adviser

Professor Heather Powell

Copyrighted by

Anna Debski

2020

Abstract

Abdominal aortic aneurysm (AAA) is a life-threatening vascular disease, characterized by abnormal dilatation of the aorta and remodeling of the elastin and collagen components of the extracellular matrix (ECM). While elastin remodeling is well characterized and is understood to dictate the vessel wall's architecture and stability, little is known about microstructural changes regarding collagen remodeling.

This study focuses on identifying characteristics of collagen remodeling in AAA which can eventually be applied to understand pathogenesis and therapeutic techniques in AAA. Studies were conducted on aortic tissue obtained from mouse models of AAA and clinical AAA tissue excised at the time of vascular surgery. Non-AAA control aortic samples from each species were also utilized. Atomic force microscopy (AFM), a high-resolution nanoscale imaging technique was used to observe the sample topography and characterize collagen fibrils. Tissues were also stained using collagen hybridizing peptide (CHP) and analyzed using fluorescent microscopy and second harmonic generation (SHG) microscopy to locate regions of healthy and degraded collagen.

Our results indicate that a significant fraction of collagen fibrils in AAA tissues departed from their native structure. These 'abnormal' fibrils had unresolvable D-period bands and a wavier, appearance. AFM analysis revealed a significant reduction in the depth of D-periods in these abnormal fibrils. Additionally, regions of abnormal collagen were located within the remodeled areas of AAA tissue and were distinct from healthy collagen regions as ascertained using CHP staining and SHG. Quantifying the amount of degraded collagen in AAA tissue and understanding the causes of abnormal collagen remodeling can provide novel insights into the ECM remodeling process in AAA and other cardiovascular diseases.

Acknowledgements

I would like to thank my research advisor Dr. Gunjan Agarwal for her continued support and guidance in my research and academic endeavors. Without her I would not have had the chance to experience the opportunities I had throughout my undergraduate career. Dr. Agarwal has provided me with great mentorship and has encouraged me throughout this entire project. She has helped me become a better student, better researcher and better engineer.

I would also like to thank Blain Jones for his time and efforts in transitioning me to this project and his continued guidance as it progressed. Without his help, the project would not have been completed.

I would also like to thank Dr. Powell for serving on my defense thesis. The classes she taught have provided me with extremely valuable lessons, both related and unrelated to academia. Throughout my time at the university, she has helped me make several tough decisions and her continued encouragement has motivated me throughout my journey.

Lastly, I would like to thank my fellow lab mates in Dr. Agarwal's lab. Their help with my project has enabled its completion. I have learned throughout my time in the lab from them and will continue to employ what they have taught me in my future experiences. It has been great working with all of them.

Vita

2016.....Bridgewater Raritan Regional High School

2016 to present.....B.S. Materials Science and Engineering, The Ohio State University

Fields of Study

Major Field: Materials Science and Engineering

Publications

Jones, B. Tonniges, J. R., **Debski, A.**, Albert, B., Yeung, D. A., Gadde, N., Mahajan, A., Calomeni, E. P., Go, M. R., Hans, C. P., Agarwal, G. Collagen fibril abnormalities in human and mice abdominal aortic aneurysm, *Acta Biomaterialia*. 2020.

Hogrebe, N., Reinhardt, J.W., Tram, **Debski, A. C.**, Agarwal, G, N., Reilly, M.A., Gooch, K.J. Independent control of matrix adhesiveness and stiffness within a 3D self-assembling peptide hydrogel. *Acta Biomaterialia*, 2018;70:110-119.

Table of Contents

Abstract.....	ii
Acknowledgements.....	iv
Vita.....	v
Fields of Study.....	v
Publications.....	v
Table of Contents.....	vi
List of Figures.....	vii
List of Tables.....	viii
Introduction.....	1
Background.....	1
Research Goals.....	3
Materials and Methods.....	3
Mice.....	3
Clinical Tissue.....	4
Atomic Force Microscopy (AFM).....	4
Collagen Hybridizing Peptide.....	5
Statistical Analysis.....	6
Results and Discussion.....	6
Conclusion.....	16
References.....	17

List of Figures

Figure 1: Verification of abnormal collagen fibrils in AAA using AFM.....	7
Figure 2: Additional examples of abnormal collagen fibrils.....	8
Figure 3: Characterization of depth of D-periods in murine aortas	10
Figure 4: Characterization of depth of D-periods in human aortas.....	11
Figure 5: Fluorescent imaging of CHP signal in murine aortas.....	14
Figure 6: SHG analysis of denatured collagen.....	15

List of Tables

Table 1: Summary of measurements of D-depth of collagen fibrils.....12

Introduction

Background

Abdominal aortic aneurysm (AAA) is a vascular disease characterized by abnormal dilations in the walls of a vessel¹, which can expand, weaken and rupture, leading to fatal internal bleeding¹. It is a major contributor to mortality in the United States⁵. AAA is characterized by remodeling of elastin and collagen components of the extracellular matrix (ECM)⁶. The current and only technique used clinically to detect AAA is through monitoring the size (diameter) of the aorta². Aortas with a diameter >5.5 cm are recommended for surgical repair while aortas with a smaller diameter are not. However, this is not a foolproof technique as some small-diameter aortas continue to grow and rupture, while some large-diameter aortas remain stable^{3,4}. The unpredictability of AAA has motivated efforts to better characterize AAA, which could potentially lead to clearer identification techniques and creation of therapeutic strategies for AAA.

The primary constituents of the ECM in the vessel wall are elastin and collagen. The quantity, organization and structure of collagen and elastin fibers control the characteristics of the vascular tissue⁷. The remodeling of collagen and elastin that occurs in AAA has an impact on the AAA growth and aneurysm rupture¹. Elastin remodeling is well understood in AAA and is characterized by elastin disruption, increased crosslinking in the medial layer and a higher degree of degradation than in healthy tissue⁸. The extent of the elastin remodeling has also been identified through ultrastructural imaging⁹. Initial remodeling is characterized by formation of porous elastin by the generation of holes throughout the tissue⁹. More intense remodeling is marked by clumps of elastin fibers and severe remodeling is identified by electron-translucent elastin⁵. Degraded

elastin is also understood to serve as site(s) for deposition of calcium phosphates affecting the vessel wall compliance¹⁰. Similar characteristics of elastin remodeling have also been identified in other vascular diseases, indicating common features across a range of diseases¹¹.

While much is understood about elastin remodeling, little is known about collagen remodeling in AAA¹². Collagen abnormalities have previously been identified at the fiber level. Scanning electron microscopy and polarized light microscopy have uncovered that adventitial collagen fibers are less undulating than control tissue samples¹³. Another technique, second harmonic generation microscopy also revealed a less prominent waviness of collagen fibers in AAA in both human and mouse models^{14,15}. However, much less is understood about the abnormalities in the sub-fiber level of collagen in AAA and other vascular diseases. The sub-fiber structure of collagen i.e. the collagen fibril is instrumental to macromolecular ECM remodeling and a determinant of the functional properties of the vessel wall and the aneurysm.

Structural changes in the collagen fibrils are well characterized in diseases characterized by collagen mutations such as osteogenesis imperfecta and Ehlers Danlos syndrome¹⁶. However very little is understood about structural changes in collagen fibrils in diseases without any underlying mutation. It is interesting to note that a few reports exist on structural changes in collagen fibrils in the dermal connective tissue of patients with vascular diseases⁹. These abnormalities include changes in fibril diameter or spacing, irregular cross-sections or lack of D-periodic banding^{17,18}. The evidence of collagen abnormalities in dermal tissues led us to hypothesize that collagen fibril abnormalities would be present in the vascular tissue in AAA.

Research Goals

The goal of this study was to identify abnormalities in collagen fibrils in AAA in order to better understand the pathology of the remodeling process. AAA tissue across two different species (mice and human) were examined using ultrastructural atomic force microscopy (AFM). Tissues were also examined for collagen degradation by using a novel reagent, namely a collagen hybridizing peptide (CHP). Fluorescent imaging and second harmonic generation (SHG) microscopy were used to identify regions of intact and degraded collagen.

Materials and Methods

Mice: All mice were handled accordingly following a protocol approved by the Animal Care and Use Committee (ACUC) at the University of Missouri (Columbia, MO). All animal research experiments adhered to guidelines established at the NIH (Guide for the Care and Use of Laboratory Animals). Only male mice were used for the study due to low occurrence of AngII-induced AAA in female mice. AngII was used to induce AAA. At 8-10 weeks, male ApoE^{-/-} knockout mice were either infused with saline or with 1000 ng/min per kg of AngII from a mini-osmotic pump that was subcutaneously inserted. For implantation of the pumps, mice were anesthetized in a closed chamber with 3% isoflurane in oxygen for 2-5 minutes. Each mouse was then removed and taped to a heated procedure board (35-37°C) with 1.0-1.5% isoflurane administered via nosecone. Proceeding 28 days, the mice were euthanized with 100 mg/kg of ketamine and 20 mg/kg of xylazine, and the abdominal aorta was then harvested. The AAA was confirmed as dilated through histological evaluations.

Clinical Tissue: Human AAA tissue was obtained following an approved Institutional Review Board (IRB) protocol from The Ohio State University from patients undergoing surgery for the removal/treatment of AAA. All tissue analysis was performed following guidelines outlined in the Declaration of Helsinki and tissue was collected after obtaining a signed informed consent form from eligible patients. Patient were being treated at the Ross Heart Hospital between the times of January 2017 and February 2020. Patients were diagnosed with AAA if aorta diameters were greater than 5.5 cm. The aorta sizes were measured using CT scans. Patients who were diagnosed with having AAA were recommended to surgery based on the guidelines presented by the Society for Vascular Surgery. Tissue collected was obtained from patients ranging from 65 to 75 years in age. Non-aneurysmal control human tissue samples were harvested from the infrarenal section of the aorta during autopsies performed within 24 hours of the time of death at the Detroit Coroner's Office. Tissue use was approved by the Institutional Review Board of Wayne University, Detroit, MI and analysis was performed following guidelines outlined in the Declaration of Helsinki. During surgery, an approximate 3 x 3 cm segment was removed from the anterior aortic sac of the vessel wall and used for analysis.

Atomic force microscopy: Tissue segments obtained previously obtained from AngII-infused mice, saline-infused mice, clinical AAA human samples and non-aneurysmal human samples were dissected and fixed in 2% glutaraldehyde. The tissue samples were then embedded in Optimal Cutting Temperature (OCT) compound and flash frozen in liquid nitrogen. Sections were stored at -80°C for future use. When used for AFM analysis of topography, the OCT embedded tissues were cryosectioned into 5 µm thick sections and mounted onto poly-lysine coated glass cover slips, washed with purified water, and air dried. The sections were then imaged using with a Multimode

AFM equipped with a JV scanner and a Nanoscope IIIa Controller. Samples were imaged using tapping mode in ambient air with NSC15 cantilevers (Mikromasch). AFM height and amplitude images were obtained at 512 lines per scan direction and a scan speed of ~ 2 Hz. The length and depth of D-periods in collagen fibrils was ascertained by section analysis of the collagen fibrils in AFM height images using the Nanoscope software.

Collagen hybridizing peptide (CHP) staining: Aorta segments obtained from mouse models were used unfixed. Human AAA tissue was fixed with 4% paraformaldehyde. The tissue samples were then embedded in Optimal Cutting Temperature (OCT) compound and flash frozen in liquid nitrogen. Sections were stored at -80°C for future use. For staining, the OCT embedded tissues were cryosectioned into $5\ \mu\text{m}$ thick sections and mounted in triplicates onto microscope slides (Permafrost) and washed with purified water. The collagen hybridizing peptide (CHP), Cy3 conjugate dye was purchased from 3Helix. Two of the three sections on the slides were stained with CHP while the third was incubated with PBS as a control. For CHP staining, a solution of $10\ \mu\text{M}$ CHP in PBS was heated at $80\ ^{\circ}\text{C}$ for 5 minutes and then quenched in an ice water bath and centrifuged. $20\text{-}50\ \mu\text{L}$ of the CHP solution (or enough to completely cover the sections) was incubated in a refrigerator overnight over tissue sections. After incubating with CHP, the samples were washed three times in PBS and then mounted using a DAPI-containing mounting medium. Slides were imaged using a Zeiss Axiovert fluorescence microscope at 20x and 63x magnifications using the tetramethylrhodamine (TRITC) and DAPI filter. For SHG microscopy, slides were imaged using an Olympus FV1000 MPE Multiphoton Laser Scanning Confocal Microscope at the Campus Microscopy and Imaging Facility (CMIF) at OSU.

Statistical analysis: Data are presented as means \pm standard deviations. Statistically significant differences in D-periodicity depth were determined using ANOVA analysis and Tukey-Kramer test performed using SAS JMP software (version 14.0). The data for each of these tests complied with the constraints of the test as validated by normality and equal variance tests. A p-value <0.05 was considered significant.

Results and Discussion

The collagen fibrils are formed by a well-defined staggered arrangement and organization of collagen monomers within the fibril resulting in a natural periodic distribution of gap and overlap regions throughout its length. This molecular packing gives rise to the collagen's characteristic D-periodic banding. Normal collagen fibrils can thus be easily identified by their well-defined D-periodicity and straight contours. A departure from these characteristic features can help identify collagen fibril abnormalities.

Atomic force microscopy was utilized to evaluate ultrastructural difference in the collagen fibril structure between healthy and AAA tissue. Normal collagen was easily identified in both saline-infused mice and in AngII-infused mice (Figure 1, A and B respectively). Similarly, normal collagen was recognized in both control human samples and AAA clinical human tissue (Figure 1, D and E respectively). However, both murine AAA and human AAA tissues also revealed a population of fibrils which exhibited structural abnormalities (Figure 1, C and F respectively and Figure 2). The abnormal collagen fibrils were characterized by D-period bands, which were compromised or unresolvable. The fibril contours were more difficult to identify as compared to normal fibrils.

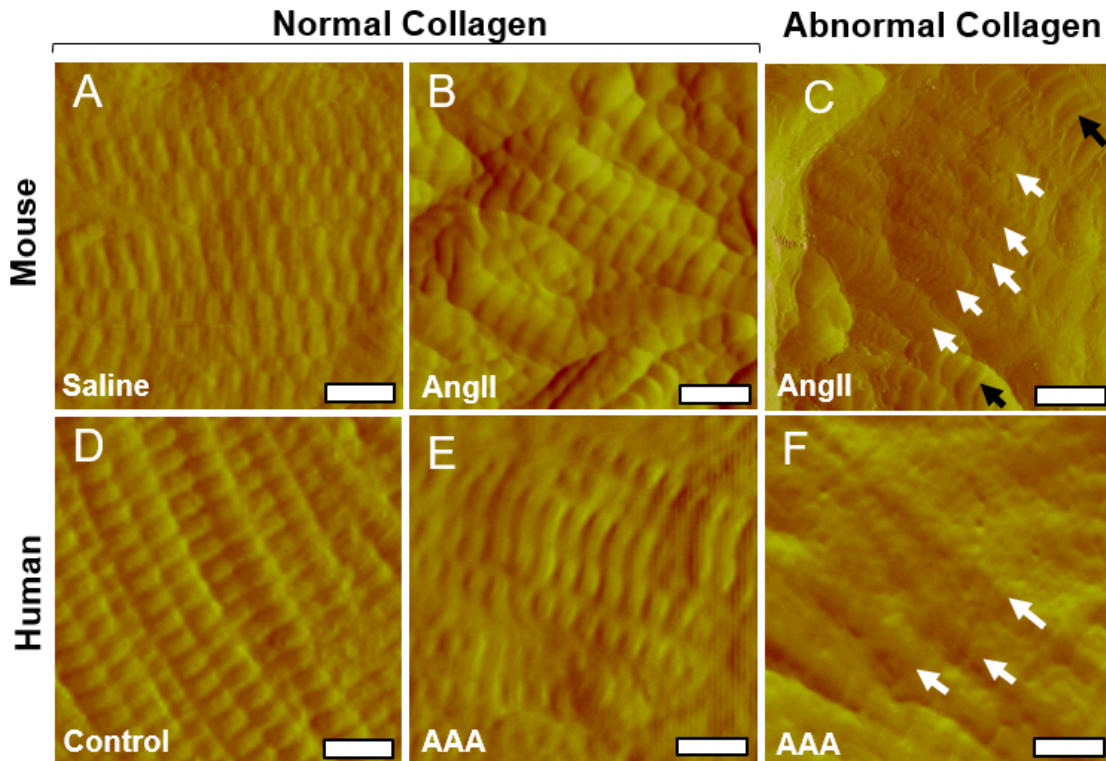


Figure 1: Normal and abnormal collagen fibrils characterized in (A-C) mouse and (D-F) human AAA using atomic force microscopy (AFM). Compromised or unresolvable D-bands were observed in AAA. Arrows (in C) indicate location and direction of normal (black) or abnormal (white) collagen. Human AAA consisted of regions with both normal and abnormal collagen fibrils. All scale bars = 200nm.

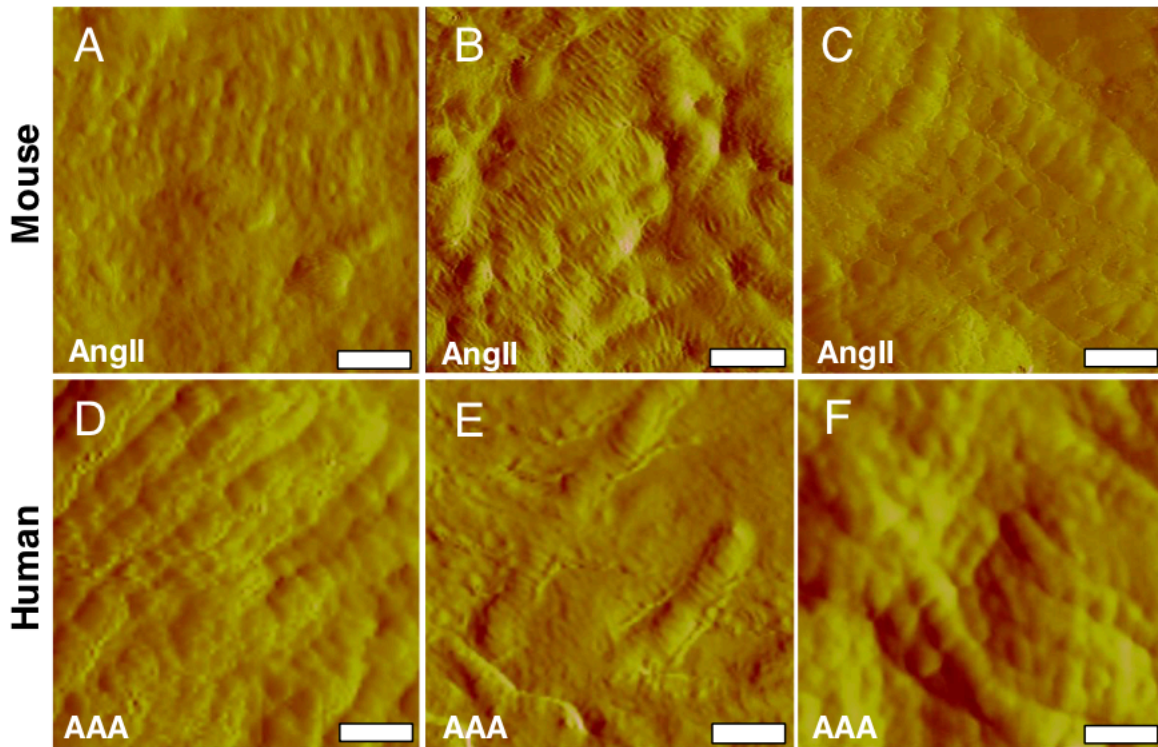


Figure 2: Additional examples of abnormal collagen fibrils in AngII-infused mice and human AAA. AFM amplitude images show adventitial collagen fibrils with disrupted or unresolvable D-bands and display collagen fibril abnormalities across multiple samples of AngII-infused mice (A-C) and clinical human AAA (D-F). All scale bars 200nm.

Since AFM can track nanoscale topography, we utilized AFM height images and their corresponding sectional profiles to analyze D-depth differences between normal and abnormal collagen fibrils. The D-period depth of three groupings of collagen was identified: normal collagen in saline-infused mice (Figure 3, A-B), normal collagen in AngII-infused mice (Figure 3, C-D) and abnormal collagen in AngII-infused mice (Figure 3, E-F). Distributions of the D-period depth indicate that normal collagen fibrils show no statistical significance in either AngII-infused mice or saline-infused mice (Tukey-Kramer test, $p=0.973$). However, abnormal collagen fibrils found in AngII-treated mice exhibited decreased D-depths (one way ANOVA followed by Tukey-Kramer

test, $p < 0.0001$). In some cases, D-period bands were compromised to such an extent that D-depth could not be identified.

AFM height images were also used to analyze differences in D-period depth in normal and abnormal collagen in human tissue. Similarly to the mouse model, D-period depth of three groups of collagen was identified: normal collagen in clinical control human tissue (Figure 4, A-B), normal collagen in clinical AAA tissue (Figure 4, C-D) and abnormal collagen in clinical AAA tissue (Figure 4, E-F). As in the mouse model, normal collagen in control human tissue and normal collagen in human AAA tissue do not present any statistically significant difference in D-period depth. However, abnormal collagen fibrils found in AAA exhibited decreased D-depths (one way ANOVA followed by Tukey-Kramer test, $p < 0.0001$). From this data, it can be elucidated that a reduced D-depth is characteristic of abnormal collagen in AAA.

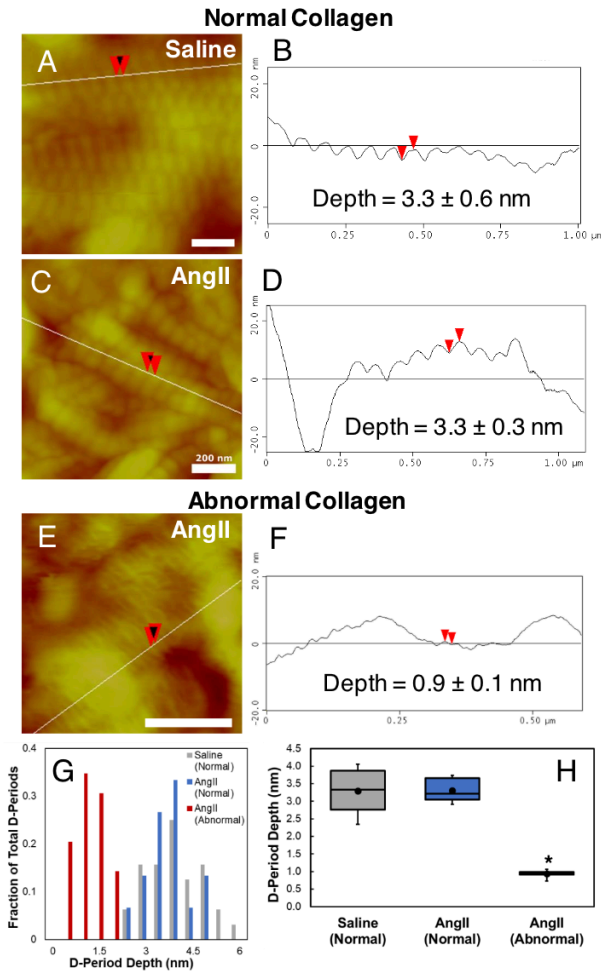


Figure 3: Characterization of depth of D-periods in collagen fibrils from murine aorta. AFM height images of normal fibrils and their corresponding section profiles for adventitial collagen in AngII-(C,D) and saline-infused mice (A,B) reveal a similar depth of D-period. However, abnormal collagen fibrils found in AngII-treated mice exhibited decreased D-depths (E,F). Scale bars are 200nm. Histogram shows the distribution of D-period depth from a representative mouse sample as indicated (G). Average depth of D-periods from all samples shows no significant differences between normal fibrils from each treatment group. However significantly reduced D-depth were observed for abnormal fibrils in AngII-infused mice (* $p < 0.0001$) (H).

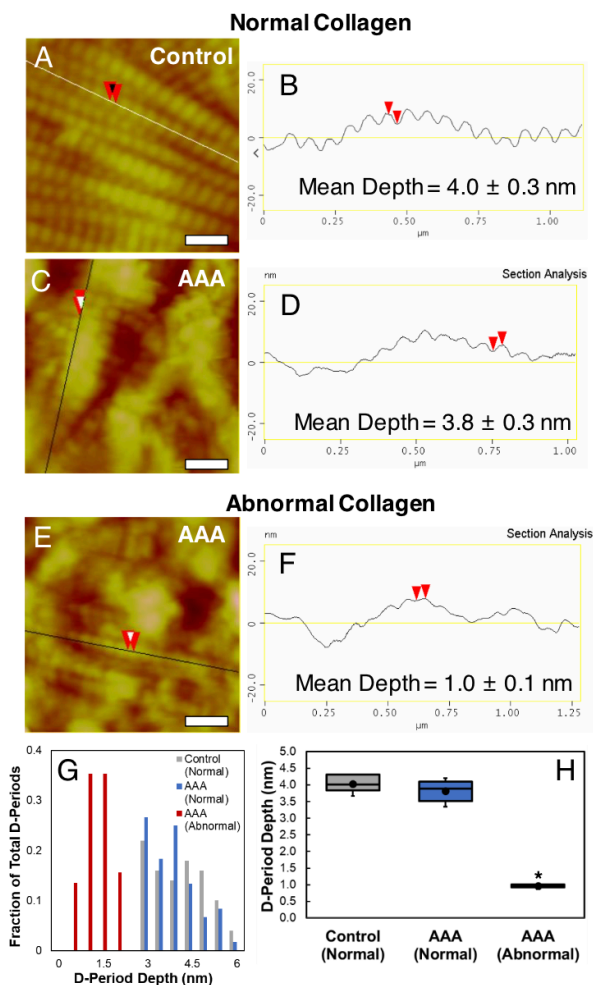


Figure 4: Characterization of depth of D-periods in collagen fibrils in human AAA. AFM height images of collagen fibrils and their corresponding section profiles are shown for normal fibrils from human control (A,B) and clinical AAA normal (C,D) and for abnormal fibrils in clinical AAA (E,F). Scale bars are 200 nm. Histogram shows the distribution of D-period depth from are presentative human sample as indicated (G). Average depth of D-periods from all samples shows no significant differences between normal fibrils from control or AAA groups. However, significantly reduced D-depth were observed for abnormal fibrils in AAA (* $p < 0.0001$) (H).

Results from the D-depth analysis for all conditions (normal collagen in saline-infused mice, normal collagen in AngII-infused mice, abnormal collagen in AngII-infused mice, normal collagen in control human tissue, normal collagen in AAA human tissue and abnormal collagen in AAA human tissue) is summarized quantitatively in Table 1. The data presented in Table 1

reiterates that there is no difference between normal collagen in control and AAA samples for both murine and human AAA models. Abnormal collagen, however, has a significantly smaller D-depth for murine and human AAA tissues. Overall, normal collagen fibrils in mouse tissue have a smaller D-depth than collagen fibrils in human tissue. Despite the differences in D-depth of normal collagen of mouse and human tissues, D-depth of abnormal human and murine collagen fibrils decrease to a similar value (~1.0 nm).

Table 1: Summary of D-depth measurements of collagen fibrils in murine/human samples.

		Depth of D-Period (nm)
Mouse	Saline (Normal)	3.3 ± 0.6 (6; 224)
	AngII-TA (Normal)	3.2 ± 0.2 (3; 57)
	AngII (Normal)	3.3 ± 0.3 (8; 111)
	AngII (Abnormal)	0.9 ± 0.1 (8; 267)
Human	Control (Normal)	4.0 ± 0.3 (6; 354)
	AAA (Normal)	3.8 ± 0.3 (6; 163)
	AAA (Abnormal)	1.0 ± 0.1 (6; 213)

Further analysis of collagen D-periodicity revealed that although banding was compromised in or unresolvable in abnormal collagen, there was no difference in the length of D-periods (66 ± 6 nm, one way ANOVA, $p=0.473$) between abnormal and normal collagen for both human and murine tissues.

Thus our AFM analysis coupled with electron microscopy analysis performed by others¹⁹ confirmed the presence of collagen fibril structure abnormalities in AAA in both human and mouse AAA. However, the source of the formation of these abnormalities is not yet understood.

Implications of these abnormalities on the functional properties of the vessel wall and stability of an aneurysm are also not yet well understood. Identifying the progression and development of abnormal collagen in AAA can lead to a better understanding of how to diagnose and treat many vascular diseases.

As another test to determine abnormal collagen we used Collagen hybridizing peptide CHP, a reagent which stains degraded collagen. CHP binds to unfolded collagen chains, and therefore is used to locate molecular denaturation of collagen and provides information on structural damage of collagen. Fluorescent imaging of CHP stained murine and human tissue was done to determine locations of degraded collagen. CHP location is represented by fluorescent regions (Figure 5, B-C, E-F). Saline-infused murine tissue (Figure 5, A) and clinical control human tissue (Figure 5, D) demonstrate no regions of intense fluorescence. However, AngII-infused murine tissue (Figure 5, B-C) and human AAA tissue (Figure 5, E-F) present with several regions of intense fluorescence. CHP analysis of aortic tissues indicates that denatured collagen is present in AAA tissue but is not in healthy tissue. Fluorescent imaging of CHP stained aortic tissue shows that collagen is denatured during the remodeling process of AAA.

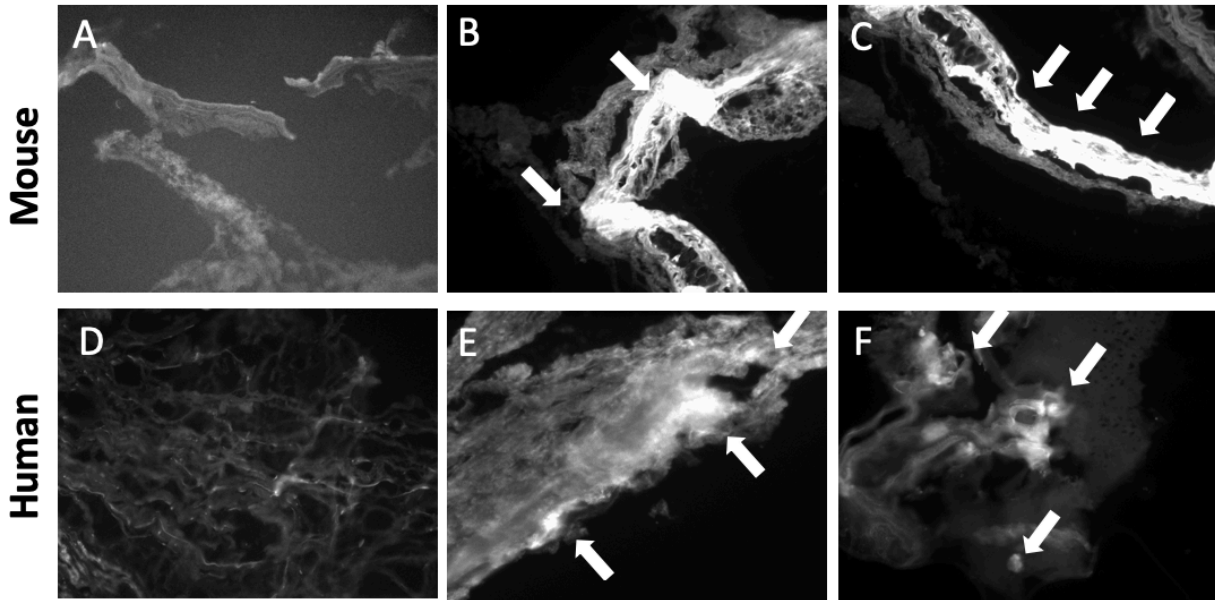


Figure 5: Normal and abnormal aorta tissue is observed for collagen degradation in mouse samples (A-C) samples. Collagen hybridizing peptide (CHP) staining was done for both saline-infused mice (A) and Ang-II infused mice (B and C) and for clinical control human tissue (D) and clinical AAA human tissue (E-F). CHP binds to unraveled or degraded collagen and can therefore be used to locate degraded collagen. Saline-infused murine tissue show no degraded collagen regions. AAA tissues present regions of degraded collagen marked with fluorescent regions indicated with arrows (B and C).

Second harmonic generation microscopy is a laser imaging technique used to visualize molecular structures of tissues. Normal collagen type I and III, which is the collagen that is found in vascular tissue ECM, naturally produces SHG contrast due to its molecular structure. On the other hand, as previously mentioned, CHP binds to denatured collagen. By simultaneously using these two detection methods, the locations of degraded and healthy collagen were able to be located. The red signal represents degraded collagen (CHP signal), the green represents healthy collagen (SHG signal) and blue represents cell nuclei (DAPI signal). The saline-infused control murine sample (Figure 6, A) demonstrated that healthy aortic tissue lacks any degraded collagen but shows evidence of healthy collagen. However, AAA murine (Figure 6, B) tissue and AAA human tissue (Figure 6, C-E) provide evidence of degraded collagen. Denatured collagen and

healthy collagen locations are clearly identifiable by their distinct fluorescent colors. Abnormal collagen regions are not co-localized with healthy collagen regions, but rather are isolated from one another. Additionally, the SHG images provide qualitative and quantitative information about the state of cell morphology and integrity. Cell nuclei are evident both in regions containing normal and abnormal collagen indicating that collagen degradation is not a result of cell death. Instead it is attributed to the collagen remodeling process of AAA.

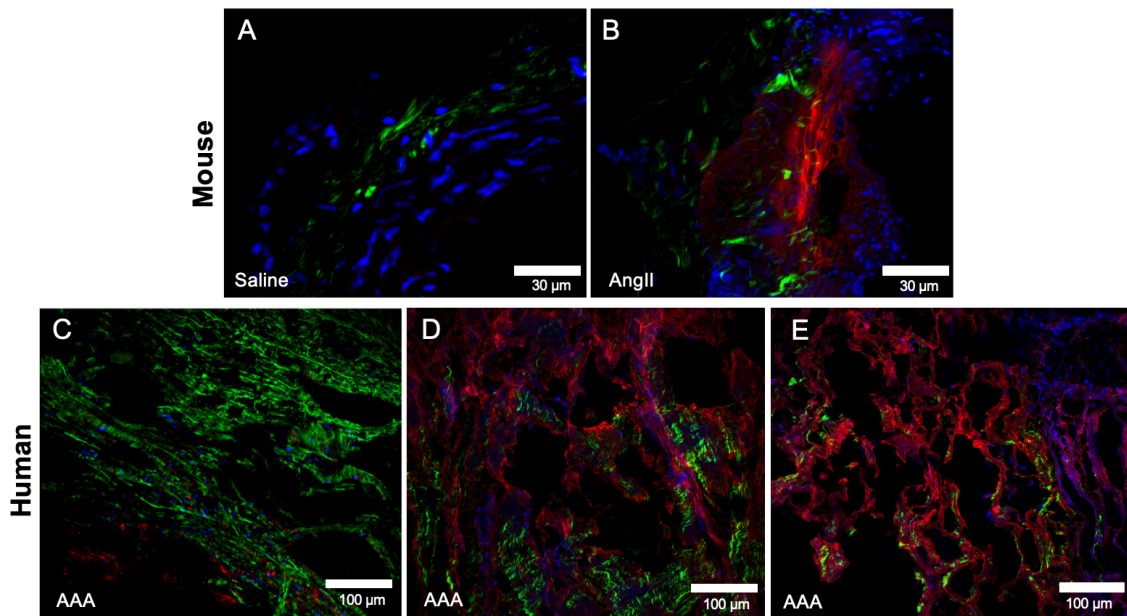


Figure 6: Images showing SHG and CHP signal. Mouse (A-B) and human (C-E) tissue is observed to determine location of degraded and healthy collagen. Blue fluorescence represents DAPI staining, red fluorescence represents CHP signal and green fluorescence show SHG signal. Healthy tissue possesses no degraded collagen (A). SHG and CHP signals demonstrate the presence of degraded collagen in murine (B) and human (C-E) AAA tissue.

SHG analysis confirmed information identified with fluorescent imaging of CHP stained tissues. Denatured collagen occurs as a result of the remodeling process associated with AAA, and is localized to sporadic pockets throughout the remodeled region of tissue. Quantification of the CHP and SHG signal can provide an estimate of the percent of abnormal and normal collagen in AAA. Understanding more about the extent of collagen degradation in AAA progression can provide insights into the collagen remodeling process.

Conclusion

In summary, abnormal collagen fibrils found in AAA present distinct differences from normal collagen found both in control samples and in AAA samples. AFM analysis demonstrated that abnormal fibrils have compromised D-period bands, undulating appearance and decreased organization. While abnormal collagen was only found in AAA tissue, normal collagen was found in both control and AAA samples. This indicated that abnormal collagen is characteristic of collagen remodeling in AAA. Quantitative analysis on compromised collagen D-period bands provided information about the differences in D-depth in normal and abnormal collagen. Normal collagen found in saline- and AngII-infused mice and in clinical control and AAA human tissue are not significantly different. Abnormal collagen fibrils, however, have a decreased D-depth present in both murine and human tissue indicating that diminished D-depth is another trait of AAA. Additionally, fluorescent imaging and SHG analysis of CHP stained aortic tissues revealed that denatured collagen is present in AAA tissues but not in control tissues. Denatured collagen and healthy collagen are located in different regions along tissue samples. Cell nuclei are located in both regions indicating that collagen degrades as a result of the remodeling process in AAA and not because of tissue death. Quantification of SHG and CHP signals in fluorescent images can provide more information about the progression of collagen remodeling in AAA. Moving forward, a technique will be optimized to do so which can provide an estimate of the percent of abnormal and normal collagen. Additionally, adjacent sections of human and murine tissue will be analyzed for AFM and CHP signal simultaneously to determine if and the type of collagen abnormalities are present in areas populated with collagen degradation. Understanding more about the remodeling process can provide novel insights into the development of diagnostics and therapeutics for AAA and other vascular diseases.

Bibliography

1. Kuivaniemi H, Ryer RJ, Elmore JR, Tromp G, Understanding the pathogenesis of abdominal aortic aneurysms. *Expert Rev Cardiovasc Ther.* 2015; 13(9): 975–987. doi: 10.1586/14779072.2015.1074861
2. McGregor, J. C., Pollock, J. G., Anton, H. C. The diagnosis of abdominal aortic aneurysms by ultrasonography., *Ann. R. Coll. Surg. Eng.* 68(1976): 388-392.
3. Nicholls, S. C., Gardner, J. B., Meissner, M. H. Johansen, H. K., Rupture in small abdominal aortic aneurysms., *J. Vasc. Surg,* 28 (1998) 884-888.
4. Singh, P., Narula, J., Molecular c=Characterization of High-Risk Aortic Aneurysms: Imaging Beyond Anatomy, *J. AM. Coll. Cardiol.* (2018). Doi:10.4172/2155-9880.1000259.
5. Phillips EH, et. al. Morphological and Biomechanical Differences in the Elastase and AngII apoE^{-/-} Rodent Models of Abdominal Aortic Aneurysms. *BioMed Research International* vol. 2015, Article ID 413189, 12 pages, 2015.
6. Basu R, Kassiri Z. Extracellular Matrix Remodelling and Abdominal Aortic Aneurysm. *J Clin Exp Cardiol.* 2013;4(8):259.
7. Borges LF, Blini JPF, Dias RR, Gutierrez PS. Why do aortas cleave or dilate? Clues from an electronic scanning microscopy study in human ascending aortas. *J Vasc Res.* 2014 Jan;51(1):50–7.
8. Tsamis A, Krawiec JT, Vorp DA, Elastin and collagen fibre microstructure of the human aorta in ageing and disease: a review. *The royal society publishing.* 2013 June.
9. Cenacchi G, Guiducci G, Pasquinelli G, Gargiulo M, Degani A, Stella A, et al. The morphology of elastin in non-specific and inflammatory abdominal aortic aneurysms. *A*

- comparative transmission, scanning and immunoelectronmicroscopy study. *J Submicroscop Cytol Pathol.* 1995 Jan;27(1):75–81.
10. Basalyga, D. M., Simonescu, D. T., Xiong, W., Baxter, B. T., Starcher, B. C., Vyavahare, N. R., Elastin degradation and calcification in an abdominal aorta injury model: Role of matrix metalloproteinases, *Circulation.* (2004). doi: 10.1161/01.CIR.0000148367.08413.E9.
 11. Brandt T, Orberk E, Weber R, Werner I, Busse O, Müller BT, et al. Pathogenesis of cervical artery dissections: association with connective tissue abnormalities. *Neurology.* 2001 Jul;57(1):24–30.
 12. Blissett AR, Garbellini D, Calomeni EP, Mihai C, Elton TS, Agarwal G. Regulation of collagen fibrillogenesis by cell-surface expression of kinase dead DDR2. *J Mol Biol.* 2009;385:902–911.
 13. G. Urabe, K. Hoshina, T. Shimanuki, Y. Nishimori, T. Miyata, J. Deguchi, Structural analysis of adventitial collagen to feature aging and aneurysm formation in human aorta., *J. Vasc. Surg.* (2015) 1–10. doi:10.1016/j.jvs.2014.12.057.
 14. J.A. Niestrawska, C. Viertler, P. Regitnig, T.U. Cohnert, G. Sommer, G.A. Holzapfel, Microstructure and mechanics of healthy and aneurysmatic abdominal aortas: Experimental analysis and modelling, *J. R. Soc. Interface.* (2016). doi:10.1098/rsif.2016.0620.
 15. D. Haskett, E. Speicher, M. Fouts, D. Larson, M. Azhar, U. Utzinger, J. Vande Geest, The effects of angiotensin II on the coupled microstructural and biomechanical response of C57BL/6 mouse aorta, *J. Biomech.* (2012). doi:10.1016/j.jbiomech.2011.11.017.

16. Jones, B. Tonniges, J. R., **Debski, A.**, Albert, B., Yeung, D. A., Gadde, N., Mahajan, A., Calomeni, E. P., Go, M. R., Hans, C. P., Agarwal, G. Collagen fibril abnormalities in human and mice abdominal aortic aneurysm, *Acta Biomaterialia*. 2020.
17. Grond-Ginsbach C, Schnippering H, Hausser I, Weber R, Werner I, Steiner HH, et al. Ultrastructural connective tissue aberrations in patients with intracranial aneurysms. *Stroke*. 2002 Sep;33(9):2192–6.
18. Hermanns-Lê T, Piérard GE. Collagen fibril arabesques in connective tissue disorders. *Am J Clin Dermatol*. 2006;7(5):323–6.
19. Orgel JPRO, Irving TC, Miller A, Wess TJ. Microfibrillar structure of type I collagen in situ. *Proc Natl Acad Sci U S A*. 2006;103:9001–9005.